Heterogeneity in Mitotic Activity and Telomere Length Implies an Important Role of Young Islets in the Maintenance of Islet Mass in the Adult Pancreas

Si-wu Peng,* Lin-yun Zhu,* Miao Chen, Mei Zhang, Di-zheng Li, Yu-cai Fu, Shen-ren Chen, and Chi-ju Wei

Multidisciplinary Research Center (S.-w.P., L.-y.Z., M.C., M.Z., D.-z.L., C.-j.W.) and Laboratory of Cell Senescence (Y.-c.F.), Shantou University Medical School, and The Second Hospital of Shantou University Medical School (S.-r.C.), Shantou University, Shantou 515063, Guangdong, People's Republic of China

Understanding the mechanisms of β-cell dynamics in postnatal animals is central to cure diabetes. A major obstacle in evaluating the status of pancreatic cells is the lack of surface markers. Here we performed quantitative measurements of two internal markers to follow the developmental history of islets. One marker, cell-cycle activity, was established by measuring expression of Ki67 and the incorporation of 5-bromodeoxyuridine. The other marker, the aging process, was delineated by the determination of telomere length. Moreover, islet neogenesis, possibly from ductal precursors, was monitored by pancreatic duct labeling with an enhanced green fluorescence protein (EGFP) transgene. We found that islets from younger animals, on average, expressed higher Ki67 transcripts, displayed elevated 5-bromodeoxyuridine incorporation, and had longer telomeres. However, significant heterogeneity of these parameters was observed among islets from the same mouse. In contrast, the levels of proinsulin-1 transcripts in islets of different ages did not change significantly. Moreover, mitotic activities correlated significantly with telomere lengths of individual islets. Lastly, after 5.5 d pancreatic duct labeling, a few EGFP-positive islets could be identified in neonatal but not from adult pancreases. Compared with unlabeled control islets, EGFP-positive islets had higher mitotic activities and longer telomeres. The results suggest that islets are born at different time points during the embryonic and neonatal stages and imply that young islets might play an important role in the maintenance of islet mass in the adult pancreas. **(*Endocrinology* 150: 3058–3066, 2009)**

Diabetes is a metabolic disease that currently affects more than 150 million people worldwide, and the number is estimated to double by the year 2030 (1). Both type 1 and type 2 diabetes are closely related to inadequate supply of insulin due to either an absolute or relative deficiency of insulin functions (2). Thus, understanding the mechanism that underlies the dynamics of β-cell mass is critical to cure diabetes.

Ironically, unlike the situation in early embryonic development (3–5), a multitude of unrelated and sometimes contradictory observations including replication, hypertrophy, neogenesis, transdifferentiation, and epithelial to mesenchymal transition have been reported regarding the homeostasis of postnatal islet β-cells in the pancreas (6, 7). β-Cell generation decreases tremendously during the first 3 wk after birth in rodents and is maintained at a low level throughout early adulthood (8). The contribution from β-cell replication and hypertrophy is well appreciated, although the role of neogenesis is still unclear (9–11). It has been estimated that more than 30% of new β-cells in neonatal rats are derived from the differentiation of progenitor cells (12, 13). β-Cell neogenesis is robust in models of pancreatic injury such as 90% pancreatectomy, partial duct ligation, or β-cell-specific destruction by an interferon-γ transgene (14–16). In addition, several long-term *in vitro* culture studies reported the generation of a progenitor population from adult pancreatic cells (17–20). Nevertheless, none of these morphometric studies were unequivocal, primarily due to the lack of reliable progenitor cell markers in the pancreas (21).

ISSN Print 0013-7227 ISSN Online 1945-7170
Printed in U.S.A.

doi: 10.1210/en.2008-1731 Received December 11, 2008. Accepted February 25, 2009.
First Published Online Mar 5, 2009
* S.P. and L.Z. contributed equally to this study.

Abbreviations: BrdU, 5-Bromodeoxyuridine; Ct, cycle threshold; DAPI, 4′,6-diamidino-2-phenylindole; EGFP, enhanced green fluorescent protein; FITC, fluorescein isothiocyanate; L, long diameter; S, short diameter.

One way to overcome this drawback is by using permanent genetic alterations to trace cell lineage during development (22). Two initial reports indicated the existence of islet progenitor cells with characteristic expression of neurogenin 3 or the ability to promote islet fission (23, 24). However, a more stringent investigation demonstrated that preexisting β-cells, instead of the stem/progenitor cells, were the main sources for the generation of new β-cells in adult mice under normal physiological conditions as well as in partial pancreatectomy (25). In addition, this group concluded in a later study that all β-cells had the same potential to replicate (26). Furthermore, by using similar tracing techniques, several groups excluded the possibility of transdifferentiation between major pancreatic cell types (27, 28). However, both the design and methodology of the above studies have been debated (6, 13). Moreover, direct challenges to the above conclusion were raised by reports that demonstrated an essential role of pancreatic stem cells in the duct for pancreas regeneration (29, 30). To complicate the situation even further, Bonner-Weir and colleagues (31) recently showed that carbonic anhydrase II-positive pancreatic ductal cells could serve as facultative progenitors that gave rise to both new islets and acini in neonates and duct-ligated mice.

In this study, we performed quantitative analyses of Ki67 and telomere length, which represent mitotic activity and cell aging, respectively, to delineate the developmental history of individual islets in the mouse under normal physiological conditions. The results demonstrated that islet neogenesis could be monitored by pancreatic duct labeling in neonatal mice. This process decreased to an undetectable level in adult animals; however, heterogeneity in terms of mitotic activity and telomere length was established among islets generated at different time points. Despite the uncertainty of the existence of islet progenitor cells, these results suggested that young islets might play an important role in the maintenance of islet mass in the adult pancreas.

Materials and Methods

Animals and materials

Eight- to 12-wk-old BALB/c mice were purchased from Shanghai Experimental Animal Center (Shanghai, China) and raised in our specific pathogen-free and air-conditioned animal facility. Biochemical reagents and antibodies were purchased from companies as indicated below: type V collagenase and 5-bromodeoxyuridine (BrdU; Sigma, St. Louis, MO); dextran T-70 (Pharmacia Biotech DB, Uppsala, Sweden); random primers (Takara, Shiga, Japan); Moloney murine leukemia virus reverse transcriptase (Toyobo, Osaka, Japan); TRIzol reagent (Invitrogen, Carlsbad, CA); 4′,6-diamidino-2-phenylindole (DAPI; Dojindo, Osaka, Japan); mouse anti-BrdU, fluorescein isothiocyanate (FITC)-conjugated goat antirabbit IgG, and FITC-conjugated goat antimouse IgG (Boster, Wuhan, China); goat antimouse insulin (Santa Cruz Biotechnology, Santa Cruz, CA); rabbit antienhanced green fluorescence protein (EGFP; Beyotime, Beijing, China); FITC-conjugated rabbit antigoat IgG (Calbiochem, La Jolla, CA); Cy3-conjugated mouse antigoat IgG (Jackson Laboratory, Bar Harbor, ME); Alexa Fluor 594-conjugated goat antirabbit IgG (Invitrogen, Frederick, MD); Cy3-conjugated sheep antimouse IgG (Sigma); and mounting fluid (Applygen, Beijing, China). All other reagents were of analytical grade.

Islet purification and quantification

Pancreatic islets were isolated from 8-wk- to 10-month-old male BALB/c mice. The mice were killed by ether anesthesia in compliance with the guidelines for the use and care of laboratory animals established by Shantou University. Islets were isolated by pancreatic duct inflation with 2 ml of 0.5% type V collagenase. Pancreases from 1 and 2 wk were harvested without inflation and chopped into smaller pieces before digestion. Digestion was carried out in a 37 C water bath for about 10 min before the enzyme was inactivated with cell culture medium. After washing, islets were purified with dextran gradient as described previously (32).

To quantify islet number and islet mass (actually islet volume in this study), the digested pancreas was suspended in 12 ml of medium supplemented with 0.05% of dithizone and subsequently allocated evenly into a six-well plate. Islets stained with dithizone in each well were counted under microscope using a ×10 objective (Eclipse TE 2000; Nikon, Tokyo, Japan). A two-dimensional scale was fitted into one of the eyepieces to facilitate the measurement of islet size. The long diameter (L) and short diameter (S) of each islet were determined for the estimation of islet volume, which was calculated by using the following equation for an elliptical sphere: volume $= \pi \times L \times S \times (L+S)/12$. Islet clusters smaller than 20 μm in length were no countered. Islets were then arbitrarily grouped into the small (30–90 μm), medium (100–160 μm), and large (≥170 μm) categories.

Real-time RT-PCR

The procedure for real-time RT-PCR has been described previously (33). Total RNA was isolated by using TRIzol reagent (Invitrogen) according to the manufacturer's protocol. Three micrograms of the total RNA was used for RT using random primers and Muloney murine leukemia virus reverse transcriptase in a total volume of 20 μl. After reverse transcription, the cDNA was diluted with H_2O (deoxyribonuclease and ribonuclease free; Toyobo) into 100 μl of which 5 μl were used in real-time PCR for proinsulin-1, cyclophilin-A, p16, Ki67, or EGFP measurement. Sequences of the specific primers and probes were as follow: proinsulin-1 forward primer, 5′-CCAGCTATAATCAGAGACCATCAG-3′, proinsulin-1 reverse primer, 5′-ACAAAAGCCTGGGTGGGTT-3′, proinsulin-1 probe, 5′-AAGCAGGTCATTGTTTCAACATGGCC-3′; cyclophilin-A forward primer, 5′-TATAAGGGTTCCTCCTTTCACAGAA-3′, cyclophilin-A reverse primer, 5′-GGACCTGTATGCTTTAGGATGAAGT-3′, cyclophilin-A probe, 5′-CAGGATTCATGTGCCAGGGTGGTGA-3′; p16 forward primer, 5′-CATGTTGTTGAGGCTAGAGAGGAT-3′, p16 reverse primer, 5′-AGTTGAGCAGAAGAGCTGCTACG-3′, p16 probe, 5′-AGAAGAGGGCCGCACCGGAATCCTG-3′; Ki67 forward primer, 5′-GCAGGTTAGCACTGTTATGAAAAC-3′, Ki67 reverse primer, 5′-GGGCCTTGGCTGTTTTACATT-3′, Ki67 probe, 5′-TGGAAGCCAAAAGAGAAAATCCTGTCAC-3′; EGFP forward primer, 5′-AAGCAGCACGACTTCTTCAAGTC-3′, EGFP reverse primer, 5′-TCGCCCTCGAACTTCACCTC-3′, EGFP probe, 5′-CATGCCCGAAGGCTACGTCCAGGAG-3′. PCR was carried out in a 96-well plate using the ABI Prism 7300 system (Applied Biosystems, Inc., Foster City, CA) with the following thermal conditions: 50 C for 2 min, 95 C for 10 min followed by 40 cycles of 95 C for 15 sec and 60 C for 1 min. The reaction for each sample was performed in triplicate. The expression level of cyclophilin-A [cycle threshold (Ct) = 18] was used for normalization. A Ct of 38 was designated arbitrarily as 1.

Telomere length measurement by real-time PCR

Genomic DNA from the β-cell line NIT-1 was harvested according to the protocol provided by the company (QIAmp DNA microkit; QIAGEN, Valencia. CA) and was used for standard curves determination. DNA from groups of islets was isolated as above. However, DNA from single islets was purified from the organic phase of TRIzol after RNA isolation.

The procedure for human telomere length measurement with real time PCR has been described previously (34) and has been modified for specific measurement of mouse telomeres (35, 36). Real-time PCRs were performed on an ABI Prism 7300 system (Applied Biosystems) using

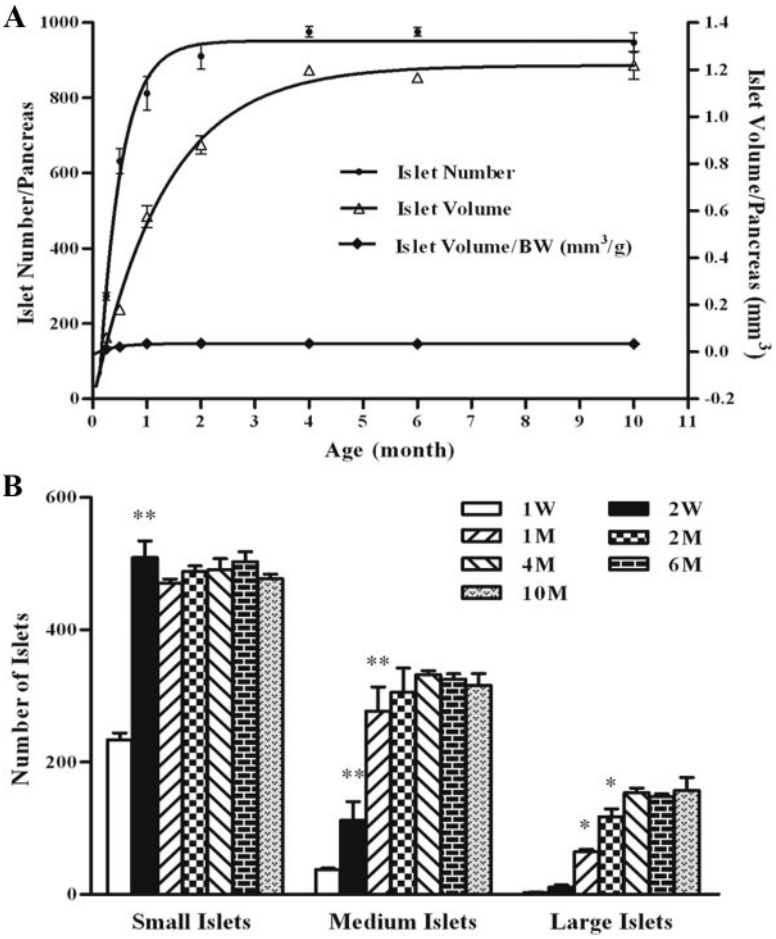

FIG. 1. Islet enumeration and size measurement in mice of different ages. Pancreases from 1 wk (W) to 10 months (M) of male BALB/c mice were isolated and digested with collagenase as described in *Materials and Methods*. A, Total islet numbers per pancreas were counted directly under a microscope and sizes were measured by using a scale fitted into one eyepiece. The volume of islets was calculated and used to evaluate islet mass. The ratio of islet volume to body weight maintained relatively constant. B, Islets were grouped arbitrarily into the small (30–90 μm), medium (100–160 μm), and large ($\geq$170 μm) categories. *, $P < 0.05$; **, $P < 0.01$ compared with that of the time point in front. At least four mice were used to determine the values at each time point in this experiment.

SYBR Green I (Toyobo). Primer sequences and concentrations for the telomere and the reference gene, 36B4, have been described by previous studies (35, 36). PCR was performed with the following thermal conditions: for telomeres, 50 C for 2 min, 95 C for 10 min followed by 40 cycles of 95 C for 15 sec, with 54 C annealing for 30 sec, followed by extension at 83 C for 30 sec; for 36B4, 50 C for 2 min, 95 C for 10 min followed by 40 cycles of 95 C for 15 sec and 58 C for 1 min. After the amplification, the Ct of telomeres was normalized to that of single-copy gene 36B4 (Ct = 18). Relative telomere length of each islet was calculated by using the following equation: $T_R = 2^{(C38-Ct)}/2^{(Ct38-Ct0)}$, where T_R is relative telomere length; Ct is the Ct of telomere; Ct0 is the highest Ct value of telomere of islets analyzed; Ct38 is cycle threshold of 38; $2^{(Ct38-Ct)}$ is relative telomere signal.

Retrograde pancreatic duct labeling

The procedure for retrograde pancreatic duct labeling has been described previously with slight modifications (37). Briefly, 2-month old male BALB/c mice were fasted for 24 h and anesthetized before laparotomy was performed through a midline abdominal incision. The common bile duct was dissected out from the connective tissue at the porta hepatis and was clipped just before it branched into the hepatic ducts. Then the common bile duct was ligated loosely at its duodenal end, and a 30-G needle was inserted into the duct through the duodenal papilla. The needle was then clipped at the duodenal orifice. Adenoviral vectors (type 5) carrying an EGFP expression cassette (Vector Gene Technology Co. Ltd., Beijing, China) dissolved in 60 μl PBS (4×10^8 pfu) containing 10% protease inhibitor (Trasylol; Bayer, Leverkusen, Germany) was injected slowly. For neonatal mice (12–14 d), the volume of the viruses was reduced to 20 μl. The abdomen was closed with suture after the needle and clips had been removed.

Immunofluorescence staining

Immunostaining was done on paraffin sections after antigen retrieval with sodium citric solution (0.01 M, pH 6.0) at 95 C for 20 min. Incubation for the primary antibody (predetermined dilution plus 1% BSA) was carried out at 4 C overnight. Staining for the secondary antibody was done at room temperature for 1 h. Samples were washed three times with PBS (5 min each wash) after antibody incubations. Ten microliters of DAPI (1 μg/ml) were added to each sample after the last wash. One drop of mounting fluid was added to the sample before it was laid over with cover slide and sealed with nail polish. Images were taken under a fluorescence microscope equipped with a charge-coupled device camera (Eclipse TE 2000; Nikon).

BrdU incorporation and detection

The procedure for BrdU labeling has been described previously (38). Briefly, thymidine analog, BrdU (100 mg/kg body weight), was injected ip twice a day for the adult mice. In some experiments, neonatal mice were injected only once 6 h before the animals were killed, or otherwise indicated.

For BrdU detection, paraffin sections of the pancreases were incubated with 0.5 M HCl at 37 C for 30 min to denature DNA after antigen retrieval. The slides were washed three times with PBS. Mouse anti-BrdU antibody (1:100 dilutions) was applied at 4 C overnight. An FITC-conjugated goat anti mouse (1:10) or Cy3-conjugate sheep antimouse IgG (1:200) was used to reveal the BrdU incorporation. For frozen sections of purified islets, the slides were fixed with 4% paraformaldehyde before staining.

Statistical analysis

All data were presented as the mean value $\pm$ SD of each group. Statistical analyses, including Student's *t* test and linear regression analysis, were carried out by using GraphPad Prism 5 (GraphPad, La Jolla, CA).

Results

New islets were generated in pancreases from neonatal mice

To investigate whether islet hyperplasia (neogenesis), in addition to islet hypertrophy, also contributed to the increase of islet mass in postnatal life, we performed a longitudinal study of islet number and size on male BALB/c mice. Consistent with previous reports (6–12), the result showed that islet mass (volume) increased about 13-fold from 1 wk to 4 months and maintained relatively unchanged thereafter (Fig. 1A). On the other hand, islet number reached a plateau earlier at 2 months and increased more dramatically, about 18-fold.

Furthermore, size distribution analysis revealed that small islets increased only for the first 2 wk after birth, whereas medium and large islets were responsible for the majority of increase during 2 wk

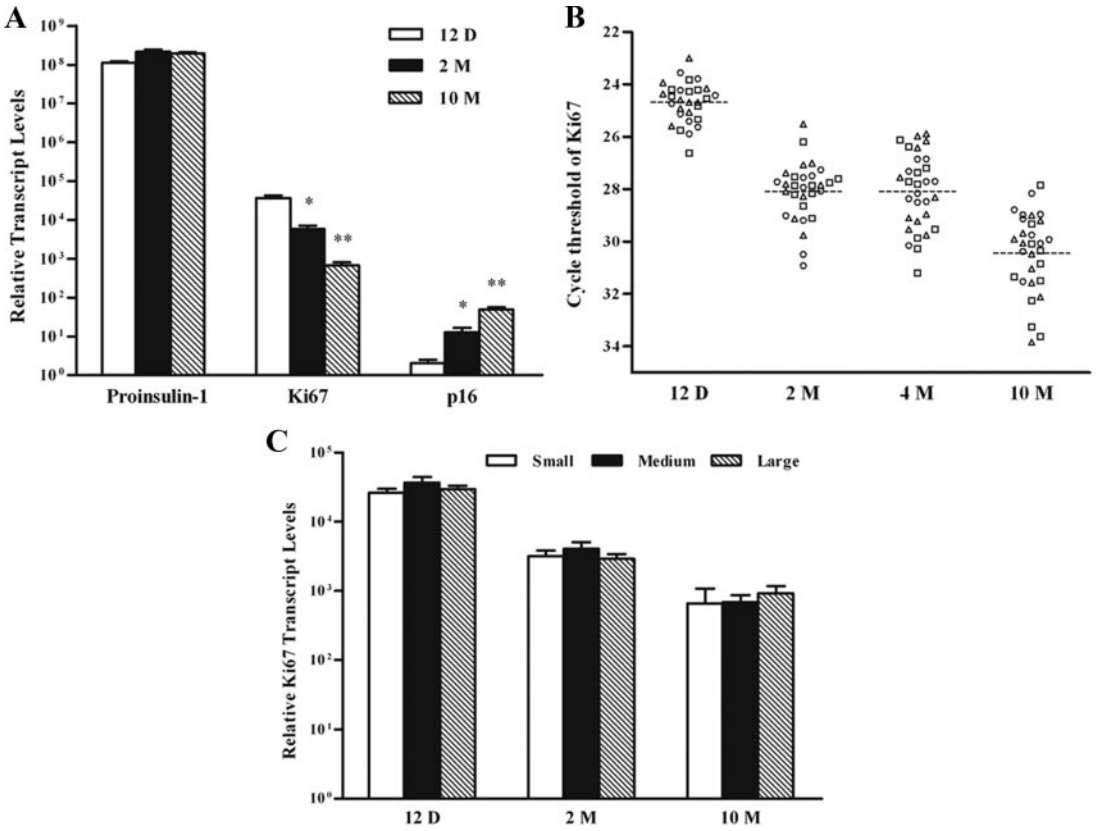

FIG. 2. Determination of proinsulin-1, p16, or Ki67 transcripts in islets from mice of different ages. The transcript levels were measured in islet mixtures (A), single islets (B), small, medium, and large islets (C) and isolated from mice of 12-d-, 2-month-, 4-month-, or 10-month-old by real-time RT-PCR. The expression level of cyclophilin-A was used for normalization (Ct 18). Relative transcript levels were calculated after designating arbitrarily Ct 38 as 1. In A and C, n = 4. In B, data in each time points represent individual islets from three mice: *triangle*, *circle*, and *square*. The *broken lines* indicate the mean values of each data set. *, $P < 0.05$; **, $P < 0.01$ compared with that of 12 d.

to 2 months (Fig. 1B). Collectively, these data suggested that both islet hyperplasia and hypertrophy were involved in the generation of islet mass in the adult pancreas. However, the source of islet neogenesis and the relationship among individual islets remained unclear.

Islet transcript levels of Ki67 decrease as mice age

Due to the lack of surface marker, we reasoned that internal characters could be used to trace the generation history of islets. The nuclear protein Ki67 has been used frequently as a proliferation indicator, whereas the cell-cycle regulator p16 is related to senescence and aging (39). Thus, we carried out quantitative analyses using real-time RT-PCR to establish a link between the expression levels of Ki67 and p16 and the developmental history of islets in the pancreas.

The results show that the transcript levels for proinsulin-1 remained mostly constant in islets isolated from mice of all ages (Fig. 2A). In contrast, islets from younger mice expressed lower levels of p16 and higher levels of Ki67 than their counterparts from older animals. Therefore, if islets in the pancreas were generated at different time points, we might be able to distinguish them individually by comparing their expression levels of p16 and Ki67.

Heterogeneity in mitotic activity could be detected among single islets

Due to the sensitivity of the method, we succeeded only with the analysis of Ki67 expression in single islets (Fig. 2B). The result demonstrated that the cycle threshold values for Ki67 had a range of about three cycles (after normalization to Ct 18 of cyclophilin-A) among islets from mice 12 d old. The range increased to about seven cycles as the animals aged to 10 months old. These results indicated that individual islets in the pancreas might indeed exist at different developmental ages.

To test whether the size of islets was also indicative of age, we measured the transcript levels of proinsulin-1, p16, and Ki67 after arbitrarily grouping the islets into small, medium, and large categories. Contradictory to our expectation, the result did not show significant differences in the expression levels of proinsulin-1, p16, and Ki67 between islets of different sizes (Fig. 2C and data not shown). A similar observation was made by another report using BrdU labeling (40).

Therefore, to directly confirm the heterogeneity in mitotic activity among single islets, the rate of BrdU incorporation was measured. The result showed that labeled β-cells rose as labeling time increased at ages 12 d and 1 month (Fig. 3A). However, BrdU staining among individual islets was highly variable in all tested conditions.

To exclude potential bias in sampling, BrdU staining on sequential frozen sections from isolated islets was used for statistical analysis of mitotic cells. The result showed that the percentage of BrdU incorporation differed by 2- to 6-fold among individual islets in neonatal 12-d-old mice. A similar degree of heterogeneity was found in islets from adult 1-month-old animals (Fig. 3B).

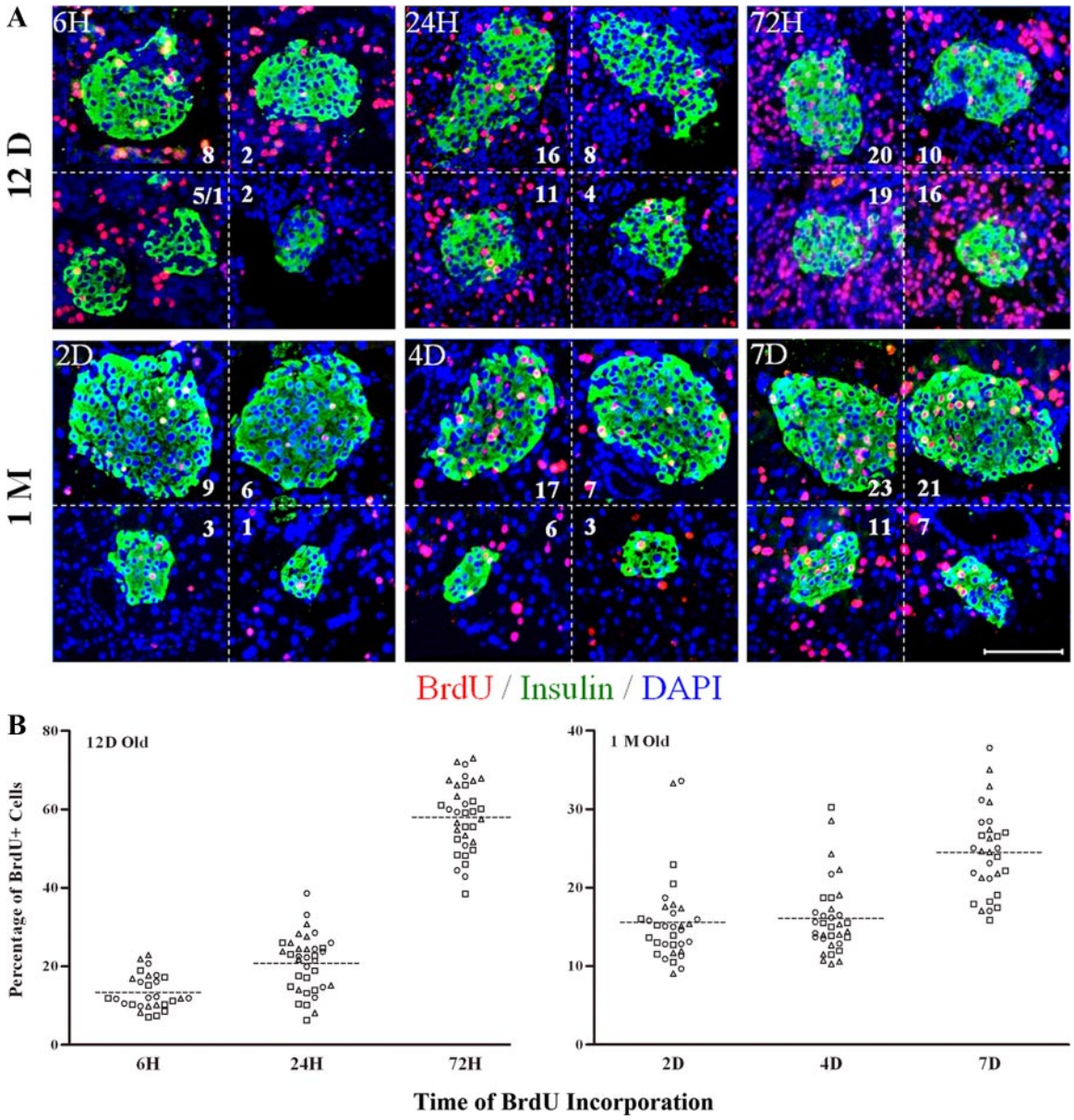

FIG. 3. BrdU incorporation and immunofluorescence staining on islets from mice of different ages. Twelve-day-old and 1-month-old mice were labeled with BrdU (100 mg/kg body weight) peritoneally for different periods of time [from 6 h(H) to 7 d(D)] before the pancreases were isolated. A, The paraffin sections were used for immunostaining of BrdU (*red*), insulin (*green*), and DAPI (*blue*). *Numbers* in the micrographs represented different numbers of BrdU-positive cells in single islets. *Scale bar*, 100 μm. B, Quantification of BrdU incorporation in individual islets from sequential frozen sections of purified islets. Data in each time points represents individual islets from three mice: *triangle*, *circle*, and *square*. The *broken lines* indicate the mean values of each data set. (n = 3).

Telomere length correlated to mitotic activity among single islets

In an attempt to find another independent marker for islet ages, we measured telomere length using real-time PCR (34–36). We first verified this newly established approach by using serial dilutions of DNA from a β-cell line NIT-1 cells. The result showed that the amplification of both the single-copy gene 36B4 and telomeres correlated linearly with the concentration of input DNA (Fig. 4A). Thereafter we performed similar analysis on purified islets from mice of different ages. Consistent with a previous report in human pancreas (41), the result demonstrated that islet telomere length decreased as the animal aged, especially during the first 2 months when islets demonstrated higher proliferative activities (Fig. 4B).

Telomere measurement was then carried out on single islets. Similar to the heterogeneity of Ki67 expression, the cycle threshold for telomeres in single islets differed by about 1.5 cycles after normalization to Ct 18 of 36B4. More importantly, the relative telomere length in islets isolated from 12-d or 4-month-old mice significantly correlated to their mitotic activity (Fig. 4, C and D). This result suggested that both the expression level of Ki67 and telomere length could be used to characterize islets at different developmental ages in the pancreas.

Newly generated islets could be traced by retrograde pancreatic duct labeling

To link higher mitotic activities and longer telomeres with younger islets further, we performed pancreatic duct labeling by

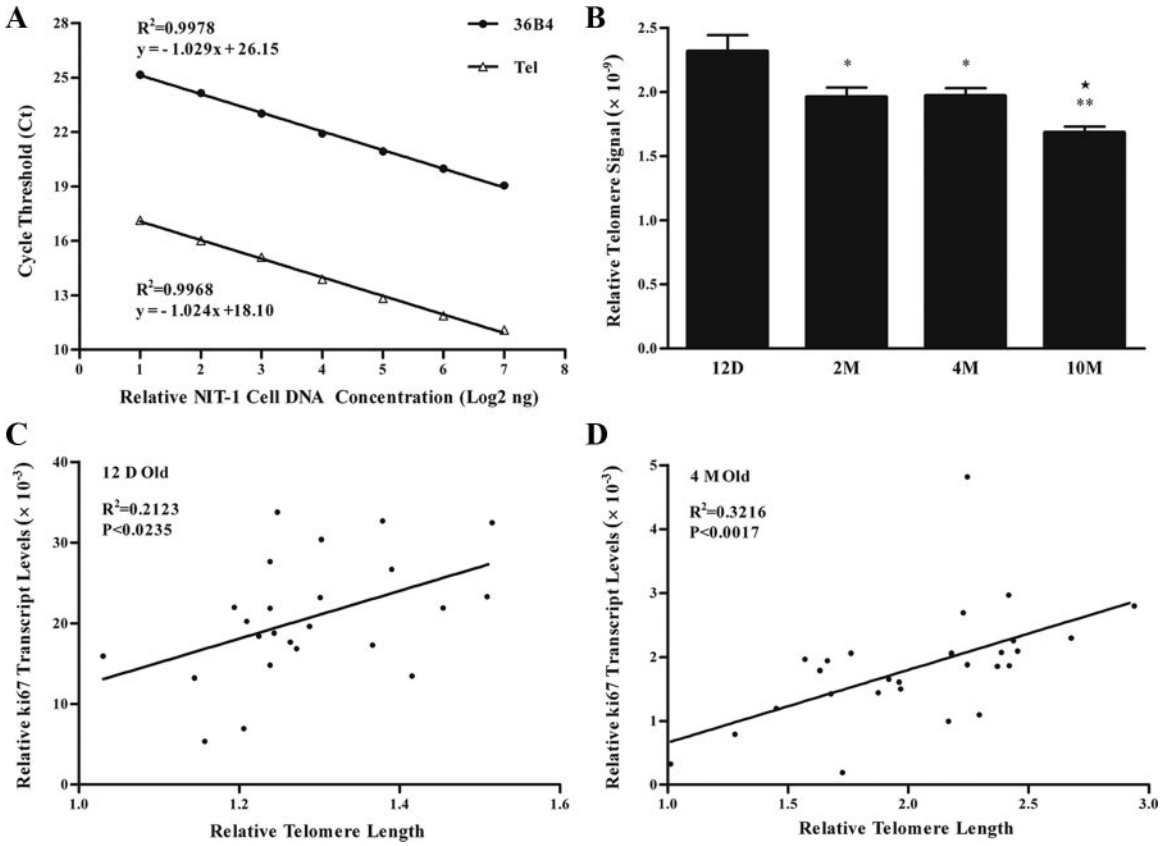

FIG. 4. Measurement of relative islet telomere length by real time PCR. A, Telomeres and 36B4 were measured using serially diluted genomic DNA isolated from β-cell line NIT-1 cells. B, Genomic DNA isolated from purified islets was used for telomere Tel measurement. C, Linear regression analysis of relative telomere length and Ki67 expression level in single islets from 12-d-old mice (12 D Old). D, Linear regression analysis of relative telomere length and Ki67 expression level in single islets from 4-month-old mice (4 M Old). Please note values of relative telomere length in C are not directly comparable with that in D. Check *Materials and Methods* for details. *, $P < 0.05$; **, $P < 0.01$ compared with that of 12 d; ★, $P < 0.01$ compared with that of 2 M (n = 4).

injecting adenoviruses carrying an EGFP expression cassette (37). The result showed that EGFP-positive ductal and acinar cells could be found extensively in neonatal as well as adult mice 1.5 d after the operation (Fig. 5A). On postoperation d 5.5, EGFP-positive β-cells could be found in the core area of a few islets in neonatal mice. On the other hand, EGFP-positive β-cells appeared only occasionally around the periphery of islets in adult pancreas during the same period, which might represent some leakage of viruses from the duct. Thus, new islets possibly generated from pancreatic duct in neonatal mice could be identified by retrograde pancreatic duct labeling.

Studies on the mitotic activity demonstrated that EGFP-positive islets tended to have more BrdU labeling than their EGFP-negative counterparts (Fig. 5B). Quantitative analysis showed that about 5.6–9.6% of BrdU-labeled cells could be found in EGFP-positive islets (Fig. 5C). In contrast, the percentage was reduced to 2.9–3.9% in EGFP-negative islets from two experimental studies. However, we failed to detect a significant difference between EGFP-positive and EGFP-negative cells within EGFP-positive islets in terms of BrdU incorporation (data not shown).

Finally, after digestion, EGFP-positive islets (constituted about 2% of total islets) were separated from EGFP-negative islets under a fluorescence microscope. The identity of islets was verified by dithizone staining. Real-time RT-PCR of the EGFP transgene was used to verify this separation (Fig. 5D). Furthermore, the analyses showed that EGFP-positive islets had higher levels of Ki67 and longer telomeres compared with their controls (Fig. 5D). Thus, these data further suggested that EGFP-labeled islets were newly generated and possibly from the pancreatic duct.

Discussion

A fundamental question regarding islet development in postnatal pancreas is whether pancreatic stem/progenitor cells exist and, if so, in which pancreatic compartments do they reside. The technical challenge to solve this issue arises from the slow turnover rates of adult β-cells (40). To exacerbate the situation, reliable surface markers are not available for the identification of potential progenitor cells in the adult pancreas (21). In this study, without genetic manipulation, we performed quantitative measurements of mitotic activity and telomere length in individual islets as a first step to estimate the existence of potential progenitor cells in normal physiology.

To achieve this, the history of islet generation in postnatal life was first evaluated by a longitudinal study. The values of islet number and volume are mostly consistently with previous reports using different methods (8, 9, 42). In addition, we found

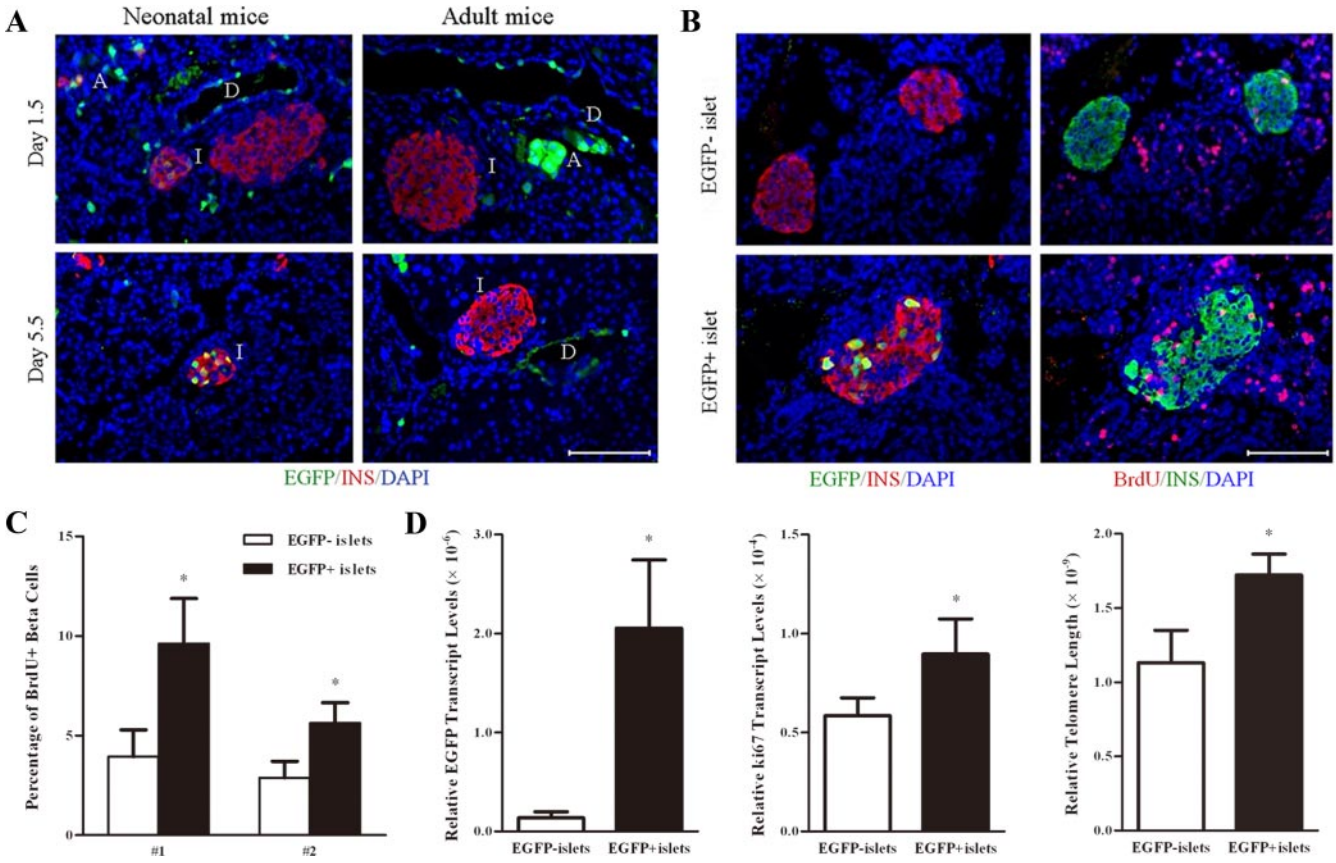

FIG. 5. Identification of newly generated islets by retrograde pancreatic duct labeling. Neonatal and adult mice were injected with adenoviruses carrying an EGFP expression cassette. BrdU was injected at 36, 24, and 12 h before the mice were killed. Panel A, Pancreases were harvested at 1.5 (*upper panel*) or 5.5 d (*lower panel*) after the operation. Paraffin sections of the pancreases were immunostained for insulin (*red*), EGFP (*green*), and DAPI (*blue*). D, Duct; I, islet; A, acinus. (n = 6). *Scale bar*, 100 μm. Panel B, Consecutive paraffin sections of the pancreases were stained for insulin/EGFP/DAPI (*left panel*) or insulin/BrdU/DAPI (*right panel*). An EGFP-labeled islet was shown on the *lower panel*, whereas two EGFP unlabeled islets were shown on the *upper panel*. *Scale bar*, 100 μm. Panel C, The percentage of BrdU incorporation was determined in EGFP+ and EGFP− islets isolated from two mice (no. 1, no. 2). Panel D, EGFP+ and EGFP− islets were hand picked under a fluorescence microscope. The ratios of EGFP, Ki67 expression levels, and telomere length between EGFP+ and EGFP− islets were determined by real-time RT-PCR or PCR. *, $P < 0.05$ (n = 3).

that the process of islet neogenesis occurred dramatically after birth and reduced to an undetectable level after 2 months. Because the apoptotic rate is minimal, β-cell replication could be the primary contributor to islet mass after 2 months (40). However, the result does not allow distinguishing the relative contribution to islet hyperplasia from the two major known pathways, namely budding from ducts and splitting from existing islets in neonates (13, 24).

The results demonstrate that mitotic activity, detected by the expression of Ki67 and/or BrdU incorporation, and the aging process, delineated by the measurement of telomere length, could be used as indicators of islet age in the mice (Figs. 2–4). Moreover, instead of being stochastic, mitotic activity of individual islets significantly correlated with telomere length (Fig. 4, C and D). Thus, the remarkable heterogeneity of these parameters suggests that islets are produced at different time points in the pancreas. It is noteworthy that BrdU incorporation remained heterogeneous, even after being labeled for up to 7 d, excluding a possible bias due to a snapshot of asynchronous mitotic events (Fig. 3A).

However, the degree of heterogeneity in terms of Ki67 expression seemed to be greater than that of BrdU incorporation in islets. Ki67 can be detected at all cell cycle stages except G_0, whereas BrdU incorporation represents cells undergoing mitosis or have passed the S stage at least once previously. Thus, these two parameters might not measure the same cell populations. Alternatively, the inconsistency might simply reflect a different sensitivity of these two approaches. In contrast, the proinsulin-1 transcripts remained mostly constant within 10 months. The result is consistent with one previous report but is contradictory to another study that showed 40% reduction over 30 months (43, 44). This could be attributed to the different methods and mice of different ages used in these studies. In any event, islet heterogeneity in this study is contradictory to the conclusions that all β-cells have similar mitotic activities in adult pancreases (26, 45).

We measured telomere length using quantitative real-time PCR, which is a simpler and faster method than other approaches (34–36). In humans it is well known that cell senescence correlates with telomere length (46). But due to the extremely long telomeres in mice, the longevity was not affected in the first three generations of mice with a deficient telomerase activity (47). In addition to cell division, telomere length is also age dependent, which can be explained by the damage caused by oxidative stress (48). Thus, the decrease of telomere length in islets from older mice could be due to increased cell division, reduced progenitor

cells, and/or accumulated oxidative stress. A combined effect of these factors on telomere length may help to explain the low R^2 number in the linear regression analysis with Ki67 (Fig. 4). It is also worth noting that a wider difference in terms of telomere lengths was observed in 4-month-old mice than that in 12-d-old mice. Nonetheless, although telomere length varies among individual animals, the significant correlation with mitotic activities clearly excluded the stochastic explanation for the heterogeneity of telomere lengths in individual islets.

This hypothesis was further supported by the study of retrograde pancreatic duct labeling (37), which allowed identification of newly generated islets in neonatal mice (Fig. 5A). Due to the nonstable transduction by adenovirus vectors, EGFP expression was significantly reduced after 1 wk. During this period, however, we could notice only very few cells around the periphery of islets in adult pancreases labeled by EGFP. Instead, in neonatal pancreases, EGFP-labeled islets had multiple EGFP-positive cells within the core area. The difference cannot be attributed simply to a potentially more leaky ductal system in the neonates. Adenovirus had been shown to have high tropism and transduction efficiency of both cycling and noncycling islet β-cells when injected iv into the mice (49). However, consistent with our observation, direct pancreatic injection of adenoviruses resulted in only few labeled islet cells around the periphery probably due to the physical blocking by the basement membrane around the islets (50). Therefore, these results suggest that islet neogenesis probably from the duct has most likely stopped in adult pancreases, whereas this process can still be monitored in neonatal animals by ductal labeling. Furthermore, the labeled islets showed higher percentages of BrdU incorporation and longer telomeres, suggesting that these islets were newly generated (Fig. 5, B–D). Although we could not formally exclude the possibility of migration of more proliferative cells from duct to islet, the failure to measure higher BrdU incorporation in the EGFP-positive cells argued against this hypothesis.

The results in this study do not provide direct evidences for the existence of islet progenitor cells and the neogenesis of β-cells (not necessary equivalent to neogenesis of islets) in adult pancreas in normal physiology. However, the observation of hormone-negative label-retaining cells suggests that cells within individual islets are also heterogeneous in terms of mitotic activity (51, 52 and our own unpublished data). Although the identity of these cells requires a more stringent investigation, we believe the results favor the existence of pancreatic progenitor cells within islets and that β-cell neogenesis has shifted from duct to islet in pancreases in the adult mice. Nevertheless, the approaches applied in this study will facilitate the searching of islet progenitor cells in adult animals in normal physiology in the future.

Taken together, the results in this study show that new islets can be generated probably from the duct in neonatal mice. The process tapers off as the animals aged. Moreover, islets generated at different time points are heterogeneous in terms of mitotic activity and telomere length. Therefore, young islets might play an important role for the maintenance islet mass in the adult pancreas. These results will be important for the development of therapeutic approaches to diabetes by identifying and targeting islet progenitor cells.

Acknowledgments

We thank Bruce M. Raaka for critical reading of this manuscript.

Address all correspondence and requests for reprints to: Chi-ju Wei, Multidisciplinary Research Center, Shantou University, 243 Daxue Road, Shantou 515063, Guangdong, China. E-mail: chijuwei@stu.edu.cn.

This work was supported by the Li Ka Shing Foundation.

Disclosure Summary: The authors have nothing to disclose.

References

1. **Wild S, Roglic G, Green A, Sicree R, King H** 2004 Global prevalence of diabetes estimates for the year 2000 and projections for 2030. Diabetes Care 27:1047–1053
2. **Cnop M, Welsh N, Jonas JC, Jörns A, Lenzen S, Eizirik DL** 2005 Mechanisms of pancreatic β-cell death in type 1 and type 2 diabetes: many differences, few similarities. Diabetes 54(Suppl 2):S97–S107
3. **Edlund H** 2002 Pancreatic organogenesis—developmental mechanisms and implications for therapy. Nat Rev Genet 3:524–532
4. **Wilson ME, Scheel D, German MS** 2003 Gene expression cascades in pancreatic development. Mech Dev 120:65–80
5. **Jensen J** 2004 Gene regulatory factors in pancreatic development. Dev Dyn 229:176–200
6. **Bouwens L, Rooman I** 2005 Regulation of pancreatic β-cell mass. Physiol Rev 85:1255–1270
7. **Bonner-Weir S** 2000 Perspective: postnatal pancreatic β cell growth. Endocrinology 141:1926–1929
8. **Scaglia L, Cahill CJ, Finegood DT, Bonner-Weir S** 1997 Apoptosis participates in the remodeling of the endocrine pancreas in the neonatal rat. Endocrinology 138:1736–1741
9. **Bonner-Weir S** 2000 Islet growth and development in the adult. J Mol Endocrinol 24:297–302
10. **Montanya E, Nacher V, Biarnés M, Soler J** 2000 Linear correlation between β cell mass and body weight throughout life in Lewis rats: role of β cell hyperplasia and hypertrophy. Diabetes 49:1341–1346
11. **Holland AM, Góñez LJ, Harrison LC** 2004 Progenitor cells in the adult pancreas. Diabetes Metab Res Rev 20:13–27
12. **Finegood DT, Scaglia L, Bonner-Weir S** 1995 Dynamics of β-cell mass in the growing rat pancreas. Estimation with a simple mathematical model. Diabetes 44:249–256
13. **Bonner-Weir S, Toschi E, Inada A, Reitz P, Fonseca SY, Aye T, Sharma A** 2004 The pancreatic ductal epithelium serves as a potential pool of progenitor cells. Pediatr Diabetes 5(Suppl 2):16–22
14. **Rosenberg L** 1998 Induction of islet cell neogenesis in the adult pancreas: the partial duct obstruction model. Microsc Res Tech 43:337–346
15. **Bonner-Weir S, Baxter LA, Schuppin GT, Smith FE** 1993 A second pathway for regeneration of adult exocrine and endocrine pancreas. A possible recapitulation of embryonic development. Diabetes 42:1715–1720
16. **Gu D, Lee MS, Krahl T, Sarvetnick N** 1994 Transitional cells in the regenerating pancreas. Development 120:1873–1881
17. **Seaberg RM, Smukler SR, Kieffer TJ, Enikolopov G, Asghar Z, Wheeler MB, Korbutt G, van der Kooy D** 2004 Clonal identification of multipotent precursors from adult mouse pancreas that generate neural and pancreatic lineages. Nat Biotechnol 22:1115–1124
18. **Ramiya VK, Maraist M, Arfors KE, Schatz DA, Peck AB, Cornelius JG** 2000 Reversal of insulin-dependent diabetes using islets generated *in vitro* from pancreatic stem cells. Nat Med 6:278–282
19. **Hao E, Tyrberg B, Itkin-Ansari P, Lakey JR, Geron I, Monosov EZ, Barcova M, Mercola M, Levine F** 2006 β-Cell differentiation from nonendocrine epithelial cells of the adult human pancreas. Nat Med 12:310–316
20. **Zulewski H, Abraham EJ, Gerlach MJ, Daniel PB, Moritz W, Müller B, Vallejo M, Thomas MK, Habener JF** 2001 Multipotential nestin-positive stem cells isolated from adult pancreatic islets differentiate *ex vivo* into pancreatic endocrine, exocrine, and hepatic phenotypes. Diabetes 50:521–533
21. **Githens S** 1994 Pancreatic duct cell cultures. Annu Rev Physiol 56:419–443
22. **Gu G, Brown JR, Melton DA** 2003 Direct lineage tracing reveals the ontogeny of pancreatic cell fates during mouse embryogenesis. Mech Dev 120:35–43
23. **Gu G, Daubauskite J, Melton DA** 2002 Direct evidence for the pancreatic lineage: NGN3+ cells are islet progenitors and are distinct from duct progenitors. Development 129:2447–2457
24. **Seymour PA, Bennett WR, Slack JMW** 2004 Fission of pancreatic islets during postnatal growth of the mouse. J Anat 204:103–116

25. **Dor Y, Brown J, Martinez OI, Melton DA** 2004 Adult pancreatic β-cells are formed by self-duplication rather than stem-cell differentiation. Nature 429: 41–46
26. **Brennand K, Huangfu D, Melton DA** 2007 All β cells contribute equally to islet growth and maintenance. PLoS Biol 5:e163–e172
27. **Desai BM, Oliver-Krasinski J, De Leon DD, Farzad C, Hong N, Leach SD, Stoffers DA** 2007 Preexisting pancreatic acinar cells contribute to acinar cell, but not islet β cell, regeneration. J Clin Invest 117:971–977
28. **Strobel O, Dor Y, Stirman A, Trainor A, Fernández-del Castillo C, Warshaw AL, Thayer SP** 2007 β-Cell transdifferentiation does not contribute to preneoplastic/metaplastic ductal lesions of the pancreas by genetic lineage tracing *in vivo*. Proc Natl Acad Sci USA 104:4419–4424
29. **Xu X, D'Hoker J, Stangé G, Bonné S, De Leu N, Xiao X, Van de Casteele M, Mellitzer G, Ling Z, Pipeleers D, Bouwens L, Scharfmann R, Gradwohl G, Heimberg H** 2008 β-Cells can be generated from endogenous progenitors in injured adult mouse pancreas. Cell 132:197–207
30. **Ackermann Misfeldt A, Costa RH, Gannon M** 2008 β-Cell proliferation, but not neogenesis, following 60% partial pancreatectomy is impaired in the absence of FoxM1. Diabetes 57:3069–3077
31. **Inada A, Nienaber C, Katsuta H, Fujitani Y, Levine J, Morita R, Sharma A, Bonner-Weir S** 2008 Carbonic anhydrase II-positive pancreatic cells are progenitors for both endocrine and exocrine pancreas after birth. Proc Natl Acad Sci USA 105:19915–19919
32. **van Suylichem PT, Wolters GH, van Schilfgaarde R** 1990 The efficacy of density gradients for islet purification: a comparison of seven density gradients. Transpl Int 3:156–161
33. **Gershengorn MC, Hardikar AA, Wei C, Geras-Raaka E, Marcus-Samuels B, Raaka BM** 2004 Epithelial-to-mesenchymal transition generates proliferative human islet precursor cells. Science 306:2261–2264
34. **Cawthon RM** 2002 Telomere measurement by quantitative PCR. Nucleic Acids Res 30:e47–e53
35. **Callicott RJ, Womack JE** 2006 Real-time PCR assay for measurement of mouse telomeres. Comp Med 56:17–22
36. **Liu L, Bailey SM, Okuka M, Muñoz P, Li C, Zhou L, Wu C, Czerwiec E, Sandler L, Seyfang A, Blasco MA, Keefe DL** 2007 Telomere lengthening early in development. Nat Cell Biol 9:1436–1441
37. **Tokui Y, Kozawa J, Yamagata K, Zhang J, Ohmoto H, Tochino Y, Okita K, Iwahashi H, Namba M, Shimomura I, Miyagawa JI** 2006 Neogenesis and proliferation of β-cells induced by human β cellulin gene transduction via retrograde pancreatic duct injection of an adenovirus vector. Biochem Biophys Res Commun 350:987–993
38. **Georgia S, Bhushan A** 2004 β Cell replication is the primary mechanism for maintaining postnatal β cell mass. J Clin Invest 114:963–968
39. **Krishnamurthy J, Torrice C, Ramsey MR, Kovalev GI, Al-Regaiey K, Su L, Sharpless NE** 2004 Ink4a/Arf expression is a biomarker of aging. J Clin Invest 114:1299–1307
40. **Teta M, Long SY, Wartschow LM, Rankin MM, Kushner JA** 2005 Very slow turnover of β-cells in aged adult mice. Diabetes 54:2557–2567
41. **Ishii A, Nakamura K, Kishimoto H, Honma N, Aida J, Sawabe M, Arai T, Fujiwara M, Takeuchi F, Kato M, Oshimura M, Izumiyama N, Takubo K** 2006 Telomere shortening with aging in the human pancreas. Exp Gerontol 41:882–886
42. **Bock T, Pakkenberg B, Buschard K** 2005 Genetic background determines the size and structure of the endocrine pancreas. Diabetes 54:133–137
43. **Perfetti R, Wang Y, Shuldiner AR, Egan JM** 1996 Molecular investigation of age-related changes in mouse endocrine pancreas. J Gerontol A Biol Sci Med Sci 51:B331–B336
44. **Wang SY, Halban PA, Rowe JW** 1988 Effects of aging on insulin synthesis and secretion differential effects on preproinsulin messenger RNA levels, proinsulin biosynthesis, and secretion of newly made and preformed insulin in the rat. J Clin Invest 81:176–184
45. **Teta M, Rankin MM, Long SY, Stein GM, Kushner JA** 2007 Growth and regeneration of adult β cells does not involve specialized progenitors. Dev Cell 12:817–826
46. **Hastie ND, Dempster M, Dunlop MG, Thompson AM, Green DK, Allshire RC** 1990 Telomere reduction in human colorectal carcinoma and with ageing. Nature 346:866–868
47. **Blasco MA, Lee HW, Hande MP, Samper E, Lansdorp PM, DePinho RA, Greider CW** 1997 Telomere shortening and tumor formation by mouse cells lacking telomerase RNA. Cell 91:25–34
48. **Furumoto K, Inoue E, Nagao N, Hiyama E, Miwa N** 1998 Age-dependent telomere shortening is slowed down by enrichment of intracellular vitamin C via suppression of oxidative stress. Life Sci 63:935–948
49. **Ayuso E, Chillón M, Agudo J, Haurigot V, Bosch A, Carretero A, Otaegui PJ, Bosch F** 2004 *In vivo* gene transfer to pancreatic β cells by systemic delivery of adenoviral vectors. Hum Gene Ther 15:805–812
50. **Wang AY, Peng PD, Ehrhardt A, Storm TA, Kay MA** 2004 Comparison of adenoviral and adeno-associated viral vectors for pancreatic gene delivery *in vivo*. Hum Gene Ther 15:405–413
51. **Duvillié B, Attali M, Aiello V, Quemeneur E, Scharfmann R** 2003 Label-retaining cells in the rat pancreas: location and differentiation potential *in vitro*. Diabetes 52:2035–2042
52. **Teng C, Guo Y, Zhang H, Zhang H, Ding M, Deng H** 2007 Identification and characterization of label-retaining cells in mouse pancreas. Differentiation 75:702–712